SPE 119895

Using Microseismic Events to Constrain Fracture Network Models and Implications for Generating Fracture Flow Properties for Reservoir Simulation

Sherilyn Williams-Stroud, SPE, Microseismic Inc.

This paper was prepared for presentation at the 2008 SPE Shale Gas Production Conference held in Fort Worth, Texas, U.S.A., 16–18 November 2008.

Abstract

Microseismic monitoring of hydraulic fracture stimulation treatments has done much to diminish the expectation of engineers and geoscientists that symmetrical bi-wing fractures extending away from the well bore from as a result of the treatment. Mapping of microseismic event locations indicates that more often, zones of high complexity form which suggest multiple rock failure mechanisms could be in play during the stimulation treatment. The complexity of the failure is further complicated, or perhaps explained, by the interaction of the perturbed stresses with existing fractures in the reservoir relative to the unperturbed stress state of the reservoir. Existing fracture planes favorably oriented for shear will fail at lower stresses than are required to create new fractures. Geologic mapping and regional to local in-situ stress information will allow informed interpretation of the resulting microseismicity patterns as well as providing predictive capability for fracturing patterns of treatments in subsequent area wells and production planning. Correlative to the improved fracture mapping is the use of the fracture interpretation as input to fractured reservoir modeling and fractured reservoir simulation. Utilizing microseismicity data not only to constrain location of fractures, but also fracture size, shape and orientation allows creation of improved fractured reservoir models based on geologic concepts and supported by the real time data.

In this paper two examples are presented from a hydraulic stimulation of North American mid-continent wells that were monitored with a surface-based geophone array. The resulting microseismicity patterns in both wells show that the fracture development was strongly influenced by pre-existing discontinuities (fractures or faults), which are easily explained by geologic and in-situ stress analysis. The fracture interpretation and microseismicity data from one example is used to generate a discrete fracture network from which fracture flow properties are created in a geocellular model. The resulting model provides a quantitative framework for production history mapping and reservoir behavior, with hard constraints for the behavior of the dominant fractures in the fracture network.

Introduction

Mapping microseismic events as indicators of fracture location and extent provides engineers and geoscientists with a tool to evaluate the success of a hydraulic fracture stimulation treatment. Often the microseismic event locations fail to outline an expected trend interpreted to indicate the fracture plane, and in many cases it is difficult to define any trend at all. The ideal case where the fracture induced by the increased fluid pressure forms symmetrical wings on either side of the borehole parallel to the maximum stress direction may in fact be the most uncommon case in the earth, as it requires unbroken brittle rock. As reservoir rock typically has undergone at least one episode of tectonic deformation, natural fractures should be expected to exist in the reservoir. The directions of growth of the induced fractures is critical to well planning, for instance, where the stimulation plan needs to avoid fracture growth into neighboring wells (Maxwell et al, 2002). Increasingly, workers are interpreting that the stimulation treatment in some reservoirs has reactivated existing natural fractures that become the primary contributors for the enhanced flow that results from the stimulation treatment (Rutledge and Phillips, 2003, Gale et al, 2007).

Microseismic event character has been described as complex when the microseisms display as a cloud of points rather than having well defined linear trends. Clouds of points are interpreted to result from microseismic events occurring on multiple interacting fracture planes during the fracture treatment, but remain difficult to interpret without supporting data such as cores, image logs, and seismic or wellbore anisotropy analysis. In cases where the supporting data are not available, using the regional geologic structure and geologic deformation history can provide a first pass qualitative probability of fracture character. The approach is to identify major structural trends that may be present in the reservoir to determine the orientations of faults that may be present near the well. Stress data from the well or neighboring wells and data from the World Stress Map database (Heidbach, 2008) was used to identify potentially active failure surfaces. Fractured reservoir modeling requires information in the scale range between the world/regional scale and the borehole meso-scale, and geostatistical approaches are often employed to generate fracture properties in this scale range. Structural analysis and strain modeling approaches provide a process-based input that may be better at identifying structural features and trends that are related to deformation than a stochastic approach (Williams-Stroud, 2006). In the examples in this paper, the microseismic events are used to condition a fracture network in the meso-scale of the reservoir where hard data have historically been lacking. Because the monitoring was done using a surface-base array of geophones, in some cases a failure mechanism could be identified which provided additional information to develop a geologic context for the interpretation of the seismic event trends. A discrete fracture network model was created using the microseismicity data to define fracture set parameters such as orientation and fracture location. The event magnitudes are used to as a fracture intensity parameter to control fracture size in a the model. Fracture flow properties generated from the fracture network can be input to a geocellular model that can be upscaled for reservoir simulation.

Geologic-base hydraulic fracture mapping

The first example of fracture complexity is shown in Figure 1. The treatment well is vertical, and the first events occur about 300 feet away from the wellbore to the south (Figure 1). As the event activity continues during the treatment, the microseisms are seen to line up along a well-defined east-west trend, but then as the treatment progresses the trend abruptly bends down to the southeast (Figure 1b). The first events occur nearer to the wellbore and form the east-west trend. As the treatment continues and events start to occur further away from the wellbore, the southwest trend develops. During the last portion of the treatment time, events continue to occur along both trends. The behavior observed in this stimulation indicates that the fluid was pumped into a nearby fault plane, and that the seismic energy generated was related to induced slip along that fault. Anisotropy analysis from crossed-dipole sonic logs measured two directions of anisotropy in the well. The fast shear direction oriented mostly west-northwest (arrow a in Figure 1b) is interpreted to result from the intrinsic anisotropy from fractures in the rock. This fracture-induced anisotropy is sub-parallel to the east-west event trend because of scatter in the fracture orientations. The microseismicity along that trend is marking just one of the fracture orientations that are present in the reservoir. The fast shear wave direction for the stress-induced anisotropy is oriented southeast and defines the maximum horizontal compressive stress direction (arrow b in Figure 1b). An east-west striking fault plane, as the one outlined by the microseismic event trends is optimally oriented for strike-slip displacement relative to that stress, and as such, the seismicity from these events is interpreted to originate from strike-slip reactivation along that pre-existing fault plane. The bend in the trend of the events, however, is inconsistent with a single failure mechanism for all events, suggesting possible fault interaction behavior that requires additional analysis.

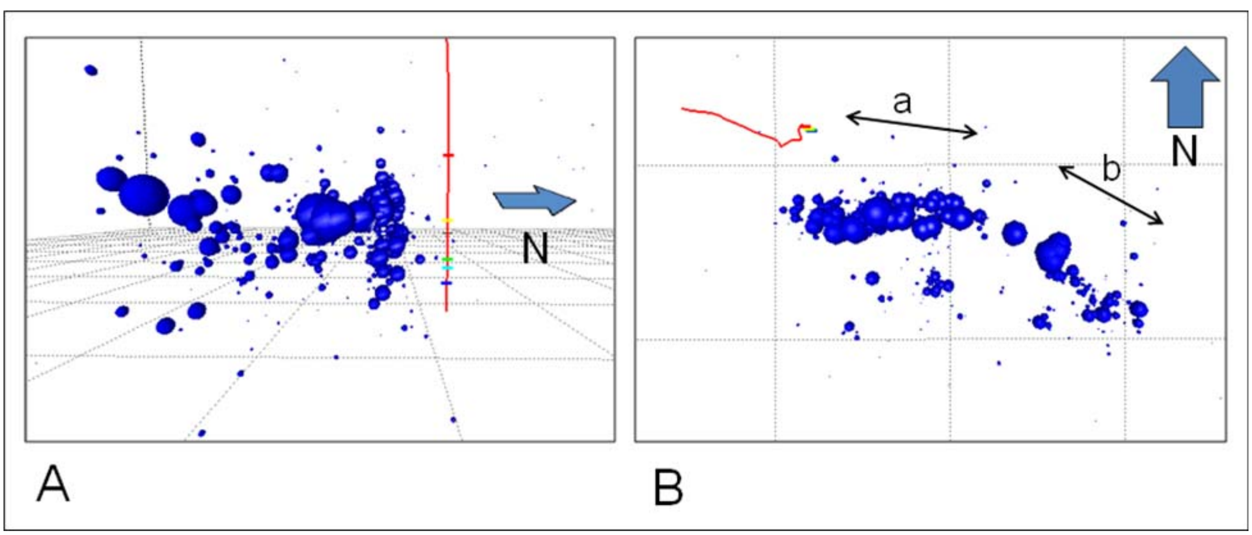

Figure 1. Microseismic events sized by relative amplitude. A. Cross sectional view of reservoir showing relationship of vertical well to events. Orientation of the view is parallel to the trend of events lined up along east-west. Distance between the well and the vertical plane defined by the events is approximately 80 meters. B. Map view, looking down into the reservoir with the vertical well in the upper left of the figure. Two event trends are clearly visible, one oriented east-west closest to the well which abruptly bends to the southeast away from the well. The arrows marked a and b show the orientations of the intrinsic fast shear wave direction (parallel to fractures) and the stress induced fast shear wave direction, respectively.

Monitoring microseismicity with a surface array provides a significant advantage to downhole array monitoring because of the capability to determine the fracture mechanisms. The broad areal coverage of the array on the surface allows analysis of the events by azimuth so that polarity change between events in different parts of the array can be determined. In comparison, downhole array monitoring can introduce a bias in the energy received by the array because the of the position of the monitoring well laterally away from the treatment well. As a result, microseismic events can only be detected from one direction and the bias can also affect the horizontal locations of events. In addition, because the downhole array is limited to the borehole, it does not have the capability to detect lateral polarity changes that can be detected by a surface array. The microseismicity data in both examples in this paper were acquired using a surface array of geophones laid out in a radial pattern around the well head, and we were able to analyze first arrival polarization changes to determine fault plane orientations. The azimuth along which the polarization changes occurred defines the strike of that plane, and is interpreted to mean that the seismic events are associated with dip-slip fault displacement (Figure 2). The events in the east-west trend and in the southeast trend were analyzed separately by azimuth, and the southeast trend revealed the largest magnitudes for a nodal plane parallel to 120^{o} azimuth (Figure 3). A single nodal plane was not determined for the east-west trend of events, indicating a different faulting mechanism for those events.

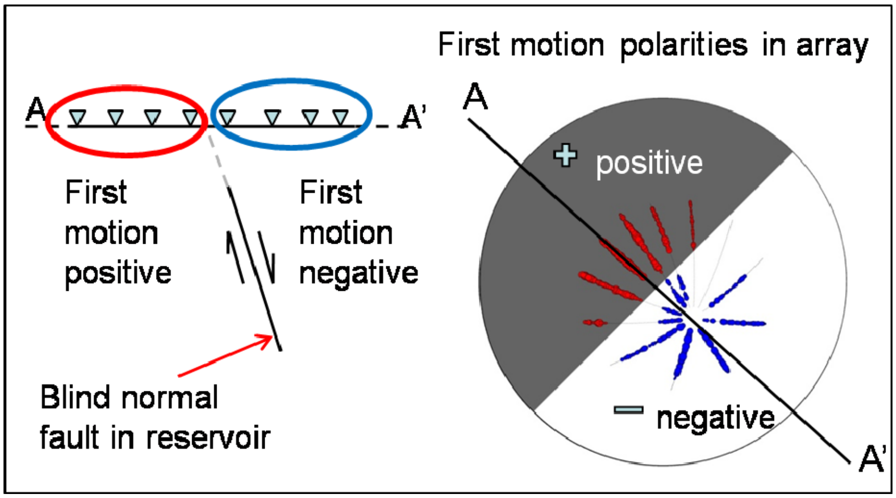

Figure 2. Diagram showing schematic microseismic surface array and relationship of nodal plane between events with positive and negative first motions as detected by array.

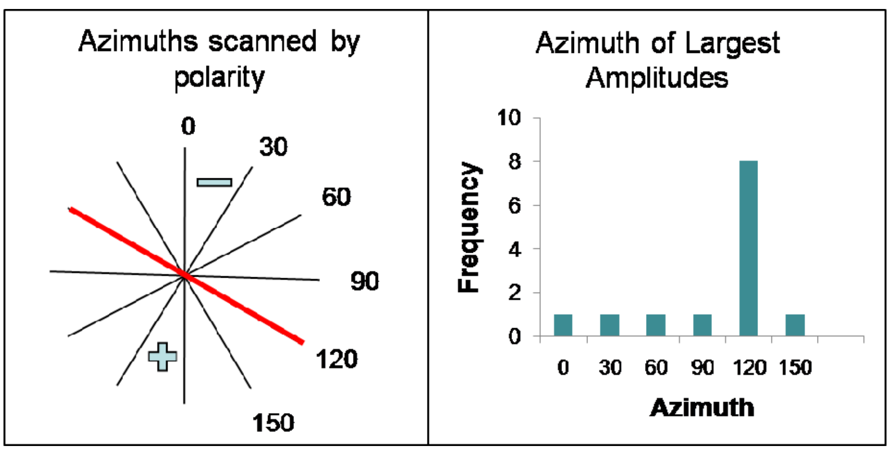

Figure 3. Relationship between number of events and azimuth of the polarity change for example data shown in Figure 1. Events at 120o azimuth have the largest amplitudes.

The fault interaction interpretation is shown in Figure 4, where the hydraulic fracturing first causes the east-west oriented fault to the south of the wellbore to slip in strike-slip, with right-lateral displacement migrating to the east until the strike-slip fault plane intersects another fault plane oriented southeast. The southeast oriented fault plane is nearly parallel to the maximum horizontal compressive stress making it no longer optimally oriented for shear (as is the east-west oriented fault), but it is optimally oriented for opening mode fracturing. In this case, a new opening mode fracture is not formed, but rather the reactivation of a pre-existing discontinuity. Overburden stress causes this discontinuity to behave as a normal fault with a component of dip-slip displacement, down to the northeast.

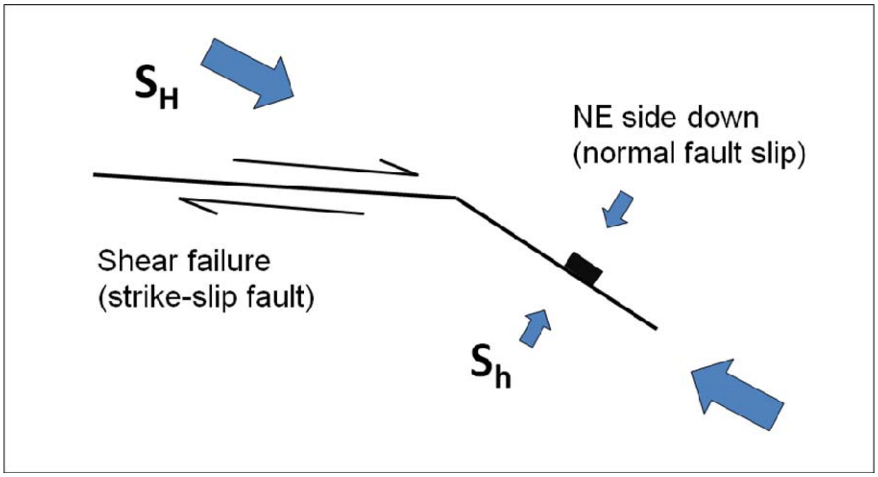

Figure 4. Geologic interpretation of event trends shown in figure 1. The strong azimuth dependence of the event amplitudes for the southeast trend is interpreted to come from dip-slip motion parallel to that trend.

Another fracturing example, also from the Mid-Continental US, is similar in that strong microseismicity trends formed during the hydraulic fracture treatment that are interpreted to indicate reactivation of existing natural fractures and faults. Figure 5 shows the results of a 5 stage hydraulic fracturing treatment in a horizontal well. During stages 1 and 2, the strongest events emanate from the wellbore between the stage 1 and 2 perforation zones, rather than from within the perforation zones. This might be interpreted to mean there was a problem with the packers between the zones, or that there are inaccuracies in the event locations, but in the subsequent stage 3 treatment, not only do the events continue to cluster around this same area (near the wellbore along the 450 meter fracture in Figure 5 B), but they also begin to occur along a line extending up to 400 meters to the west of the wellbore oriented west-southwest. The asymmetry of this line relative to the wellbore and the concentration of events along this line instead of in the location of the perforations indicates the reactivation of an existing fracture or fault. Very limited microseismic activity occurred during stage 4 except for one area of strong events west of the wellbore. All of these events occurred within a narrow time frame commencing approximately 30 minutes after the start of pumping for that stage and although these events are not on the same line, they define a similar trend to the events from stages 1-3. Events from the fifth and final stage of the treatment are the most symmetrical about the wellbore. The first events from stage 5 occur 30 to 60 meters to the west of the well and subsequent events cluster about the wellbore before the remaining events for this stage extend away from the wellbore on both sides to define a trend 360 meters in length. Although this trend could be considered a “well-behaved” nearly ideal hydraulic fracture, it is more or less parallel to the other trends from the previous stages that were not so well behaved, and is also interpreted to indicate a pre-existing fracture or fault.

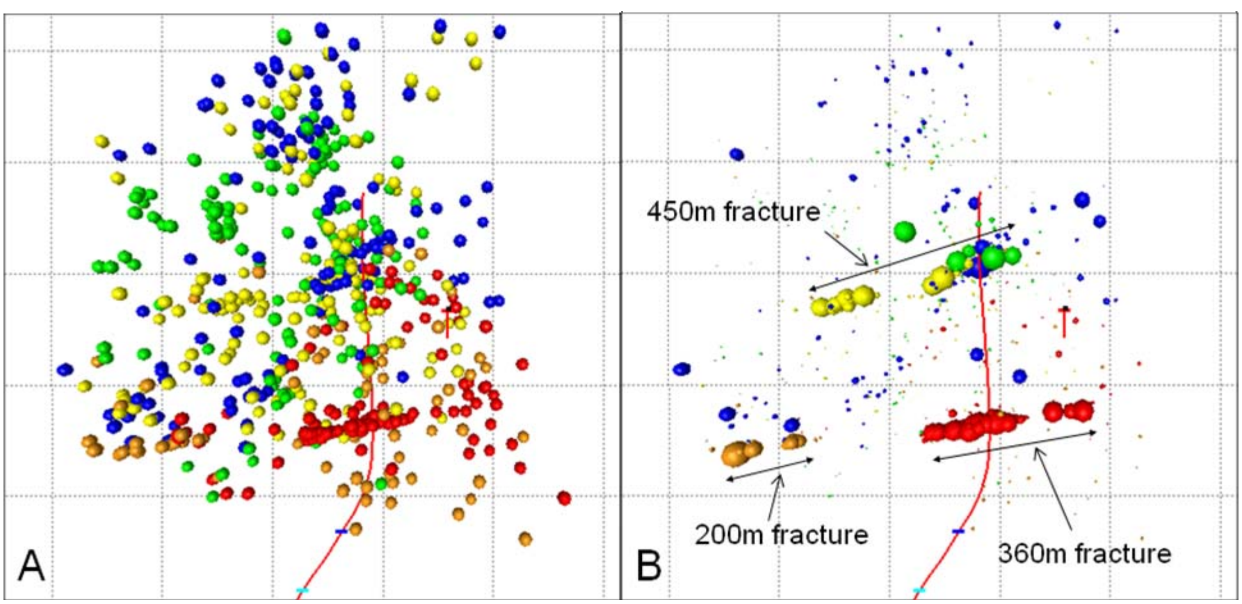

Figure 5. Two views of the microseismicity imaged from a hydraulic fracture treatment of a horizontal well. A. shows the event locations colored by stages: stage 1 = blue, 2 = green, 3 = yellow, 4 = orange, 5 = red. B. The same events sized by relative amplitude showing more clearly the fracture trends outlined by the strongest events.

In order to place the event interpretation in a geologic context, we consider the regional stress regime in this part of the mid-continental US. Maximum horizontal stresses reported from the World Stress Map Project (Heidbach, 2008) are oriented primarily east-northeast, but there is significant variability in the region with some measurements indicating a maximum horizontal stress direction west-northwest. Variations in orientations of the maximum stress could be caused by proximity of the stress measurement location to major faults. An examination of horizons about the reservoir shows that there a number of NE oriented normal faults approximately 0.6 miles (1km) to the north of the well (Figure 6).

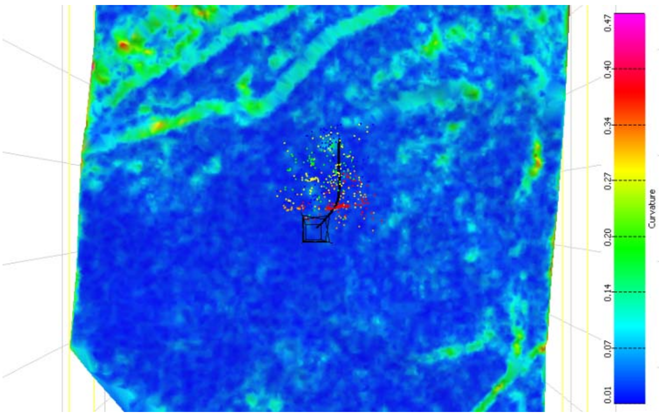

Figure 6. Top of the reservoir horizon colored by curvature (dip) Showing trend of major normal faulting north of the reservoir. The 80^o stimulation treatment fracture trend is visible just to the north of the well derrick symbol, outlined by red dots.

Curvature analysis of the horizon shows the trend of the faults 45 to 60 degrees northeast, with dip-slip displacement down to the northwest. The microseismic events define a trend at an angle approximately 25 degrees from the fault trend. If the effective stress in the reservoir is east-northeast (roughly sub-parallel) to the faults, then faults in this orientation may be expected to be presently critically stressed, meaning they are in an orientation that is likely to slip (Zoback, 2007). As the strike of these faults varies along their length, the response to the rock along their length will also vary, so that in some locations sub-seismic features may develop in order to accommodate slip. The trends of the microseismic activity in this well are within the range of orientations that could be reactivated with shear displacement in either east-northeast oriented compressive stress or west-northwest oriented compressive stress.

Using stage 3 events, the polarity of the first motion of high amplitude events was determined to reverse along a plane oriented parallel to the trend line of the events. The polarity difference could be due to dip-slip along those planes, strike-slip, or any direction of oblique slip in-between, but in either case shear failure in some direction along this plane is indicated. The availability of anisotropy information from the borehole (as in the first example above) would allow a determination of the mostly likely sense of slip for fractures in this well.

Fractures from microseismic events

The relationship between the seismic moment and the size of a fault plane on which slip occurs can be used to make a rough estimate of the fracture size associated with each microseismic event. The seismic slip or rupture occurs on patches along the large fracture surface at different locations and different times during the hydraulic fracturing treatment so that the entire fracture does not rupture at once. The seismic moment is defined as:

$$M_0 = \mu S d \qquad (1)$$

Where μ = rigidity, S = fracture area, and d = displacement. The assumptions for size of the fracture plane are guided by the length and height of the microseismicity trends that are interpreted to define the fracture planes. The events in stage 5 of the second example occur along a trend that is approximately 360m in length and 120m high (Figure 5). The location of an individual microseismic event is assumed to be in the center of a slipped patch along that fracture plane. Barton and Zoback (1994) calculate the magnitude of the stress drop on a slipped fault plane by modeling borehole breakout rotations in image logs. They model the full in-situ stress state in the borehole and relate the fault displacement stress drop to the amount of breakout rotation and the size of the fracture is related to the length of the rotated breakout interval in the borehole. However, without in-situ stress and/or rock strength measurements, as in the example used in this paper, the magnitude of the stress drops and slip displacements associated with an individual event are unknown. It is not possible to make a direct calculation of the slipped patch size, but a range of possible slipped patch sizes can be derived from the measured seismic moment M_0 and Sd (slip surface area * slip displacement) can then be calculated using equation (1). Barton and Zoback (1994) calculated slip patch areas in the range of 1 to 60 meters, so an intermediate value, 10 meters, can reasonably be used for this example. The value for rigidity can be derived from the density and the shear wave velocity, and a typical for sandstone is 1.8×10^{10} N/m. The largest magnitudes in this example are 10^6 Nm, and occur along the 80^o azimuth trends of the fractures. Many smaller amplitude events are imaged outside of these trends. These smaller events are interpreted to be seismic slip on much smaller fractures within the reservoir that are also favorably oriented for slip under the perturbed stress state of the hydraulic fracture treatment.

The model approach used to create fractures with the resulting parameters involves populating a geocellular grid with a value that defines a fracture occurrence probability. The probability value, P32 (fracture area/volume) in a particular cell of the grid defines the likelihood of a fracture to be generated in that grid cell. The size of the fracture assigned to that cell is defined by a power-law probability distribution so that small fractures are more likely than large fractures. The size range used here is 10 to 500 meters (to include fractures having lengths equal to the longest fracture trend imaged in the example), with an aspect ratio of length to height = 3. The result is large fractures that span the length of the higher amplitude event trends that define the fractures. Figure 7 shows two realizations of discrete fractures based on the events sizes and locations, one with fractures generated by the using amplitudes directly as P32, and the other with fractures generated by using the square root of the amplitude value as P32. Fracture flow properties (permeability tensor and connectivity) can be generated from the modeled fractures for input to reservoir simulation.

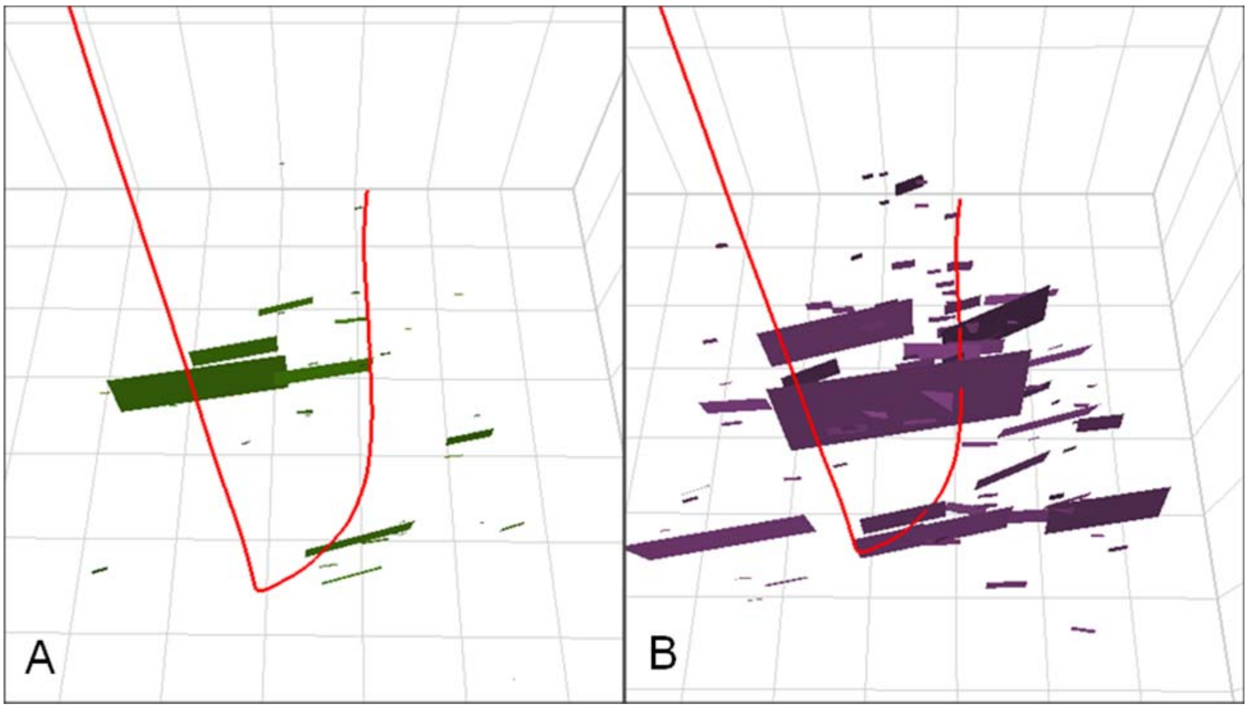

Figure 7. Discrete fracture model generated from the microseismic event locations. Event amplitude was used to control fracture location by using it as an intensity measure, and fracture sizes were controlled by the relationship between the amplitude and the seismic moment. A. fracture intensity = event amplitude. B. fracture intensity = square root(event amplitude).

Implications for reservoir modeling

The result of the discrete fracture modeling is a significant improvement over fracture generation by stochastic methods which involve using data at the wells to extrapolate the fracture character between wells. The fracture character of the reservoir is illuminated by the event locations, and using reasonable values for slip and fracture surface area, a geologically realistic fracture model can be generated that is constrained by hard data at distances of several hundred meters away from the wellbore. The fractures defined by the microseismic events also directly identify transmissive fracture orientations within the reservoir providing additional constrains for permeability calculations. When developing the reservoir history match using fracture inputs, the reservoir model can be adjusted to match by changing only the poorly-constrained parameters, size and slip magnitude, thus reducing the uncertainty of the model.

In the second hydrofracture treatment example of this paper, some of microseismicity zones appear with the strongest events at some distance from the well, with no strong events along the fracture trend that connects that energy to the well. Interpretation of the clusters of events that do not appear to originate from the well where the treatment pressure is maximum suggests some aseismic fluid flow to that area of the reservoir. The small events that occur throughout the volume away from the main fracture trends may be locations of either smaller fractures or fractures that are oriented so that they fail with less energy than those along the main fracture trends. Modeling these small events in the reservoir model as separate fracture set of small fractures with more scatter in their orientation provides additional constrains for calculating permeability between the main treatment fracture trends.

Conclusions

Microseismic events analyzed in the context of the geologic setting of their treatment reservoirs can be used to generate and constrain fracture models. Understanding the geologic context allows interpretation of the created fractures that includes sense of slip, so that the fracturing mechanism information can then be used to understand the sources of seismic energy and fractures can be more accurately modeled. Microseismicity monitoring done with a surface-based array generates a broad coverage of the area around the treatment well and also provides information that allows determination of the fracture mechanisms associated with the microseiemicity. The fracture size can be quantitatively derived from the micro earthquake energy associated with the events. The uncertainty associated with discrete fracture network models generated by stochastic or other modeling methods is greatly reduced by utilizing the locations of the larger seismic events generated in the hydraulic fracture treatment, providing much better constraints for fracture size and orientation. Previous to having microseismicity as a size and orientation constraint, discrete fracture models have had notoriously high uncertainty relating to these parameters, and as a result, in the history-matching phase of the project they lacked sufficient guidance for which parameters to tweak to improve the history match. Imaging hydraulic fracture treatments and generating discrete fracture network models from the microseismicity data provides a base for modeling the effectiveness of the stimulation. This methodology can also be applied to the full reservoir model by using the microseismicity imaged from reservoir production and injection modeling.

Acknowledgements

I would like to thank BJ Hulsey and Jo Kilpatrick for processing the data and helping me to understand the results, and Leo Eisner for explaining how to apply seismic energy principles to microseismicity data and for many helpful comments that improved the manuscript. I would also like to thank Devon Resources and Petro-Hunt for permission to use their data.

References

Barton, C. and Zoback, M. (1994): Stress perturbations associated with active faults penetrated by boreholes: Possible evidence for near-complete stress drop and a new technique for stress magnitude measurement, Journal of Geophysical Research, vol. 99, no. B5, pp 9373-9390.

Gale, J.F., Reed, R.M., and Holder, J. (2007): Natural fractures in the Barnett Shale and their importance for hydraulic fracture treatments, American Association of Petroleum Geologists Bulletin, vol. 91, no. 4, pp. 603-622.

Hanks, T. C. and Kanamori, H. (1979): A moment magnitude scale, Journal of Geophysical Research, vol. 84, no. B5, pp 2348-2350.

Heidbach, O., Tingay, M., Barth, A., Reinecker, J., Kurfeß, D., and Müller, B.(2008): The 2008 release of the World Stress Map (available online at www.world-stress-map.org).

Maxwell, S.C., Urbancic, T.I., Steinsberger, N., and Zinno, R. (2002): Microseismic imaging of hydraulic fracture complexity in the Barnett Shale, Proceedings Society of Petroleum Engineers Annual Technical Conference, San Antonio, 2002, SPE 77440.

Rutledge, J.T., and Phillips, W.S. (2003): Case History: Hydraulic stimulation of natural fractures as revealed by induced microearthquakes, Carthage Cotton Valley gas field, east Texas, Geophysics, vol. 68, no. 2, pp. 441-452.

Williams-Stroud, S., Griest, S., and Meddaugh, S. (2007): A geologic strain and reservoir attribute-based discrete fracture network (DFN) model of the Humma Field, Partitioned Neutral Zone, American Association of Petroleum Geologists Bulletin, Annual Meeting 2006, Houston, Texas, Program Abstracts, vol. 90.

Zoback, M. (2007): Reservoir Geomechanics, Cambridge University Press, 449 pp.